Available online at www.CivileJournal.org

Civil Engineering Journal

Vol. 6, No. 12, December, 2020

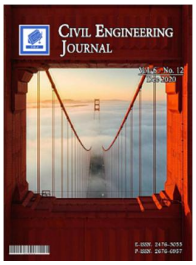

New Approach for Simulating Reinforced Concrete Walls in Quasi-static Loading

S. Benakli [a*], Y. Bouafia [b], M. Oudjene [c], K. Benyahi [b], A. Hamri [b]

[a] *Conservatoire National des Arts et Métiers, Paris, France.*

[b] *University of Tizi-Ouzou, UMMTO, BP 17 RP 15000, Tizi-Ouzou, Algeria.*

[c] *Department of Civil and Water Engineering, Laval University, Quebec, Canada.*

Received 27 February 2020; Accepted 24 November 2020

Abstract

The main objective of this article is to apply a simplified model to simulate the overall behavior of a reinforced concrete wall without the need to explicitly represent the reinforcing bars in the model nor the progressive degradations of the concrete in tension. The model takes into account the fictitious laws of the material, in order to estimate the capacity of the studied model and its performance to simulate the complex behavior of concrete. The law of the fictitious behavior of reinforced concrete tie rods is based on the shape of the adhesion curve between steel and concrete. Relationships covering the cracking stage up to the elastic limit of steel are proposed according to the properties of concrete and steel materials, the percentage of steel. An analytical computational model is then implemented in the Matlab programming language. Necessary transformations for the integration of the law of fictitious average behavior of steel in the Abaqus software were carried out thus making it possible to make a considerable advance from the point of view of validation of the developed law. The general formulation of the tension law applies to sections where the reinforcements are distributed so that the resistance of the entire section is mobilized. Hence the need to introduce an effective area around the rebars for the application of the fictitious tension law to reinforced concrete walls. Numerical simulations have been validated using an example of reinforced concrete wall subjected to a quasi-static loading. Load-displacement responses are compared and the numerical results approaches well the experimental one. By using the law of the fictitious diagram of the concrete and by defining the effective tensile zone of the wall, the model makes it possible to save a considerable time of calculation compared to a traditional calculation in EF on Abaqus.

Keywords: Reinforced Concrete; Fictitious Law of the Tie; Steel-concrete Adhesion; Effective Area of the Tie.

1. Introduction

It is well known that the tensile strength of concrete is generally neglected when it comes to dimensioning and stress checks. However, it is important to consider the contribution of concrete in tension for a better prediction of the behavior of reinforced concrete structures. The problem of the contribution of tensioned concrete between cracks and steel / concrete adhesion has been widely studied in the literature in the context of reinforced concrete tie rods leading to the formulation of different laws for the fictitious average behavior of steel. However, a certain number of parameters influencing the fictitious average behavior of steel remains to be studied and so far we do not see the transfer of this type of law to the scale of the structure under various loading conditions (other than traction).

* Corresponding author: benakli.s@gmail.com

http://dx.doi.org/10.28991/cej-2020-03091622

On the other hand, the numerical simulation of reinforced concrete structures requires the explicit representation of concrete and rebar, the two materials being modeled separately using appropriate behavior laws, including the damage variables concrete in compression and in tension. Even if this modeling method is practical and satisfactory, it requires a considerable calculation effort for the reinforced concrete elements.

The objective of this work is to develop the global behavior of reinforced concrete structures without the need to explicitly request the reinforcing bars in the model nor the progressive degradations of the concrete in tension.

In order to achieve this, the law of fictitious average behavior of the reinforced concrete tie proposed by Bouafia and Saad et al. (2014) [1], has been developed. By considering the balance of forces in a cross section of a reinforced concrete tie rod, the law of adhesion-slip can be used to establish the equations governing the slip between the tie rod reinforcement and the concrete. Thus, the average relative elongations of steel and concrete between two successive cracks can be calculated. The objective is to deduce the fictitious average constitutive law of steel and concrete in tension during the cracking phase according to the mechanical properties of the two materials and the percentage of reinforcement considered.

The innovation of this work is that integrating the fictitious average behavior law of concrete in the Abaqus software will allow us to get rid of the explicit representation of the rebars in the model but also of the progressive degradations of the concrete in tension.

First, the fictitious law of the reinforced concrete tie rod is developed, an analytical calculation model is then implemented in the programming language Matlab. Then, a finite element modeling is carried out with the Abaqus calculation code and introducing the fictitious tie rod model. Finally the law developed is validated in the case of a quasi-static loading on a reinforced concrete wall.

2. Behavior Law Adapted for Fictitious Steel

The present work proposes to establish the relationship between the applied tensile load and the average deformation ε_{cm} of a reinforced concrete element subjected to traction. The behavior law (stress-strain curve) can be obtained by dividing the total tensile load by the equivalent and homogenized cross-section of the concrete.

The law of adhesion - slip τ (g) adopted by the European Concrete Committee (CEB) [2] is used to establish the equations governing the slip between reinforcement and concrete in a reinforced concrete "tie rod".

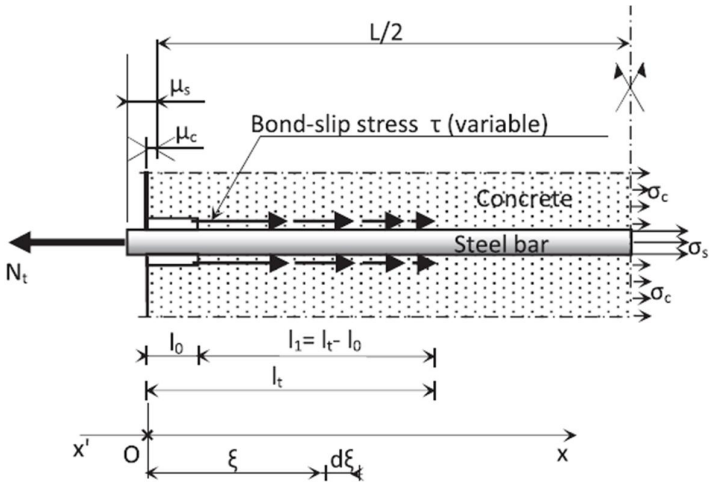

Figure 1. Relative slip g (= μ_s–μ_c) and distribution of the bond-slip shear stress

The total introduction length is noted l_t. The length l_0 represent the disturbed zone and it is taken here equal to $l_0 = \delta l_t$ ($\delta = 0.10 \sim 0.20$) [3]. The effective introduction length is $(l_t - l_0) = (1 - \delta) l_t$. The differential Equation 1 which governs the relative slip g, between steel and concrete is written as follows:

$$\frac{d^2 g}{dx^2} - \frac{p}{A_s E_s \overline{\rho}} \tau(x) = 0 \quad (1)$$

This relationship is used to establish, in the domain $[l_0,\ l_t]$, the different expressions $\varepsilon_c(x), g(x), \tau(x)$ and $\varepsilon_s(x)$ as a function of x along the effective insertion length l_t. If the effective introduction length is considered as $l_1 = l_t - l_0$, the solution of the differential Equation 1 is given by Saad (2011), Guo et al. (2018) and Mourlas et al. (2017) [4-6]:

$$g(x) = \theta^{1/(1-\alpha)}[l_1 - x]^{2/(1-\alpha)} \quad (2)$$

Where: $\theta = \frac{\beta_1^2(1-\alpha)^2}{2(1+\alpha)}$; $\beta_1 = \sqrt{\frac{k_1 p}{E_s A_s \overline{\rho}}}$; $k_1 = \frac{\tau_1}{g_1^{\alpha}}$

The variation in the bond stress at the steel-concrete interface is written then as follows:

$$\tau(X) = k_1\theta^{\alpha/(1-\alpha)}[l_1 - X]^{2\alpha/(1-\alpha)} \quad (3)$$

It is assumed that the behavior of a reinforced concrete element subjected to traction follows three main phases (Figure 2), namely a linear elastic phase (branch OA), an inelastic cracked phase (branch AC) and an elastic cracked phase (CB) [7, 8].

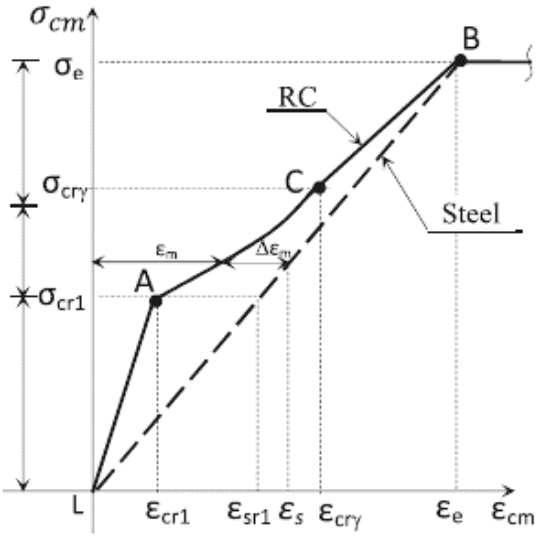

Figure 2. Stress-deformation relationship of a reinforced concrete tie rod

After the appearance of the first crack, relations are established for a reinforced concrete tie-rod by considering two cases:

- After cracking, and during crack propagation (Stage IIa) when the crack spacing remain greater than the total introduction length l_t, the main values of the relative elongations of steel and concrete are calculated and are noted respectively ε_{smt1} and ε_{cmt1}.
- At crack stabilization (Stage IIb) or during crack propagation when the total introduction length cannot develop, the main values are calculated and noted $\varepsilon_{sm\overline{\lambda_1}}$ (orε_{sma1}) for steel and $\varepsilon_{cm\overline{\lambda_1}}$ (orε_{cma1}) for concrete.

Thus, according to the loading level, and with these main values of the relative elongations, the fictitious diagram of the reinforced concrete tie rod can be drawn.

Table 1. Mean values of the relative elongations for the different stages of the fictitious diagram

Linear elastic stage	Inelastic cracked stage	Elastic cracked stage
Before crack initiation, the behavior of the RC element is regarded as homogeneous linear elastic material	It starts at the onset of the first crack. As the applied tensile force is progressively transmitted to the concrete there is a crack propagation. This stage stops when the cracking becomes stable	This stage is characterized by the stability of cracking. As the tensile loading increases, the opening width of cracks increases
$\varepsilon_{cm} = \varepsilon_{cr1} = \varepsilon_s = \frac{\sigma_c}{E_c} = \frac{\Delta L}{L} = \frac{N_t(1-\overline{\rho})}{E_s A_s}$ $\overline{\rho} = 1/\left(1 + \frac{n\rho}{1-\rho}\right)$	$\varepsilon_{cmt1} = (1-\delta)(1-\overline{\rho})\frac{1+\alpha}{2}\varepsilon_{sf}$ $\varepsilon_{smt1} = \left[\delta + (1+\delta)\left(1 - \frac{1+\alpha}{2}\right)\overline{\rho}\right]\varepsilon_{sf}$	$\varepsilon_{cmt\overline{\lambda_1}} = (1-\delta)(1-\overline{\rho})\frac{1+\alpha}{2}\varepsilon_{sfa1}$ $\varepsilon_{smt\overline{\lambda_1}} = \varepsilon_{sf} - \left[(1-\delta)\left(\frac{1+\alpha}{2}\right)\overline{\rho}\,\varepsilon_{sfa1}\right]$

The following algorithm (Figure 3) summarizes the method to be used to calculate the average relative elongations of steel and concrete. These average values will be used to determine the fictitious diagram of steel (and concrete). This diagram is then transformed into an average behavior relation of reinforced concrete. Please refer to the Benakli et al. (2018) study [8] for a better understanding of the development of the law of fictitious behavior of steel.

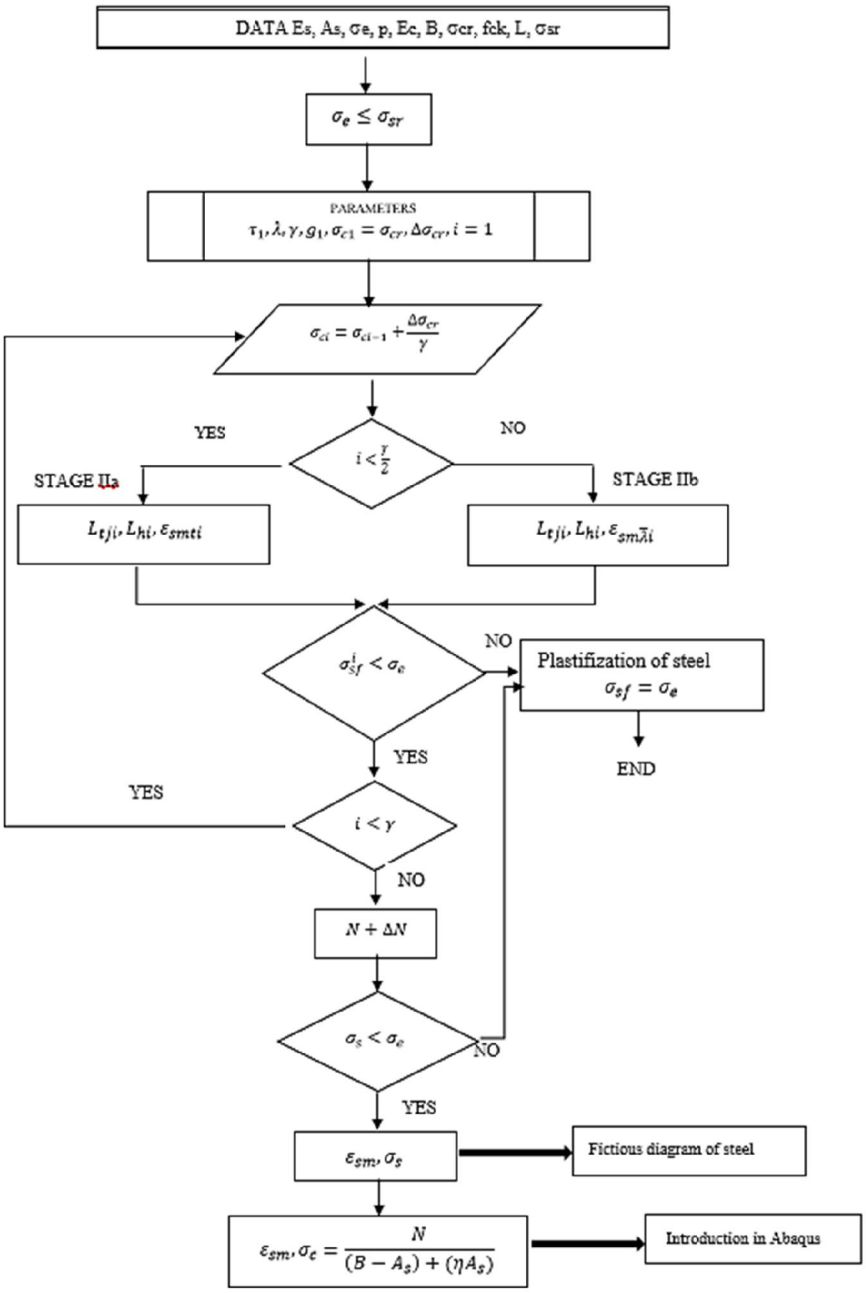

Figure 3. General calculation algorithm [7]

Therefore, an analytical model of computation is proposed. It is implemented in the programming language Matlab, in order to confront the fictitious behavior law with experimental results. The interactive side of the language facilitates the introduction (or correction) of the various data and parameters. The diagram is finally introduced into the constitutive law used in the Abaqus software.

3. Numerical Simulation of a Reinforced Concrete Wall

3.1. Modeling Strategy

The specimen of reinforced concrete wall chosen for the digital simulation is the model SW21, one of the sails tested by the experimental companion of Lefas and Kotsovos (1990) [9]. This wall is of rectangular cross section, and tested under monotonic quasi-static loading. The wall is 650 mm in length, 1300 mm in height, and 65 mm in thickness. The geometrical characteristics of the wall are summarized in the figure (Figure 4).

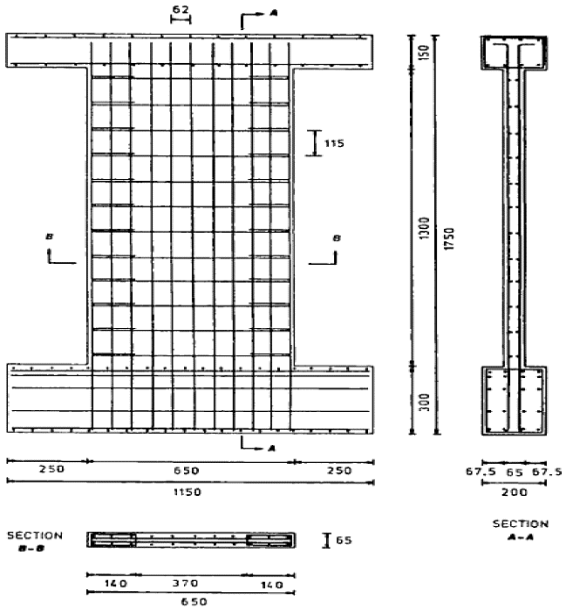

Figure 4. Details of the geometry and reinforcement of the Lefas wall (mm) [9]

In order to best represent the advantage of the fictitious law of the reinforced concrete tie, the choice fell on two approaches of modeling in finite elements:

- The first approach consists in representing concrete by solid linear hexahedron elements in 3 dimensions with a reduced point of integration (C3D8R) and in using the model Concrete Damage Plasticity (CDP) [10] included in the Abaqus software [11, 12], to represent the law of behavior in compression and traction of concrete with damage. As long as the reinforcements are represented in a discrete way using elements of lattice with 2 nodes (Truss element T3D2), and are modeled by an elastoplastic law of steel. We will call this approach "Model 1".
- The second approach for its part consists in representing only the geometry of the concrete always by 3D solid elements but without the reinforcements. The contribution of the reinforcements is then implicitly taken into account by the fictitious constitutive law of the concrete in tension integrated in the model of the concrete. This approach will be called "Model 2".

The wall is subjected to a compound bending. We want to identify the stretched part of the BA element to be taken into consideration in the “Model 2”. The question therefore arises: What is the part to which we are going to apply the law of behavior of the fictitious tie rod?

3.2. Effective Area for the Application of the Fictitious Law of the Tie Rod

This adaptation does not directly affect the law of the tie itself, but the effective area on which it must be applied. This concept has already been used in similar contexts. It also appears in the Model Code 90 CEB-FIP [2] from which the formulation below is derived. The general formulation of the law of the tie applies to sections where the reinforcements are distributed so that the resistance of the whole section is mobilized [13].

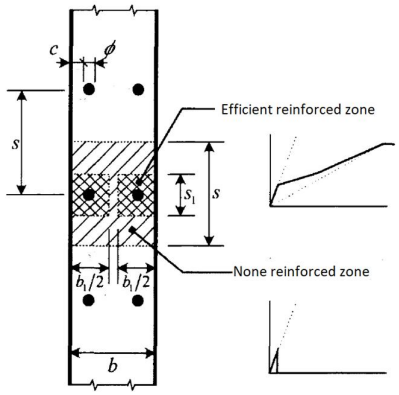

Figure 5. Principle of defining the effective zone of the application of the law of the tie [13]

In the direction of the thickness of the concrete wall considered, we generalize to any number of layers [2, 13]:

$$b_1 = n \,.\, 2.5 \,.\, (c + 0.5\phi) \nsucc b \tag{4}$$

$$s_1 = 2.5 \,.\, (c + 0.5\phi) \nsucc s \tag{5}$$

Where:

b = wall thickness

s= bar spacing

b_1 = effective thickness

s_1 = height of the effective zone in the wall plane

c= coating

ϕ = bar diameter

n = number of reinforcement plies - usually 2

Hence, for the calculation of the behavior law of the tie rod, an effective concrete area which is calculated as follows:

$$A_{ceff} = A_{cbrut} \frac{b_1}{b} \frac{s_1}{s} \tag{6}$$

3.3. Numerical Simulation

The wall is simulated numerically using Abaqus. The modeling approach is done in two duly described ways.

- **Model 1**

As described above, the concrete behavior law is defined by the CDP model. The parameters of the concrete model in uni-axial behavior (uni-axial stress-strain and damage-strain curves) were determined using experimental data.

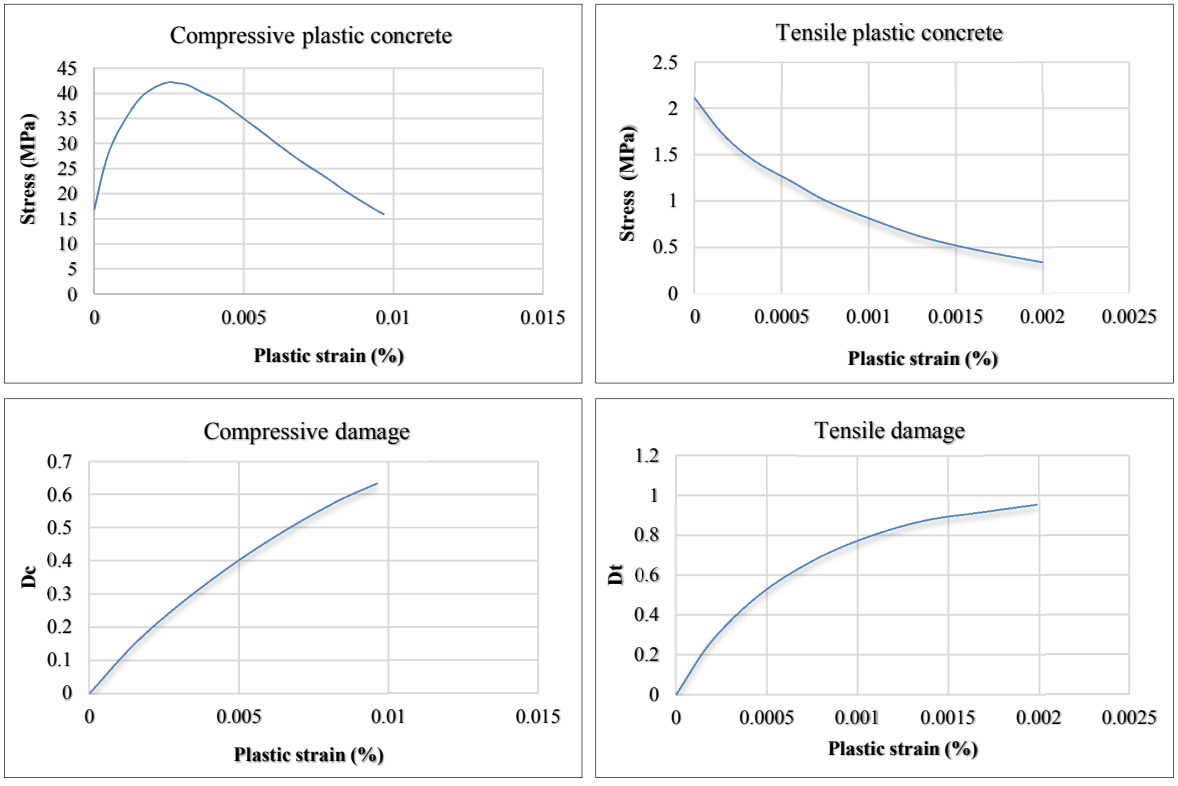

Figure 6. Uni-axial stress-strain and damage-strain curves of concrete in compression and tension (model1)

The steel bars and stirrups are modeled in elasto-plastic materials with the respective elastic constraints for the different steels; a module Es = 210GPa, and a fish coefficient ν = 0.3.

- **Model 2**

For the wall, we have represented a stretched part of the web of the wall SW21 (hatched area in Figure 7), by means of an effective area A_{ceff} = 7604.295 mm² and therefore a percentage of reinforcements ρ = 2.8%.

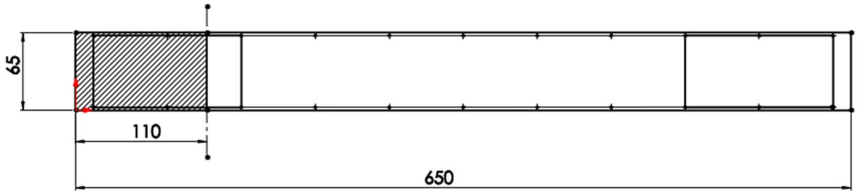

Figure 7. Part of the web of the wall SW21 taken into account for the establishment of the fictitious diagram of the concrete

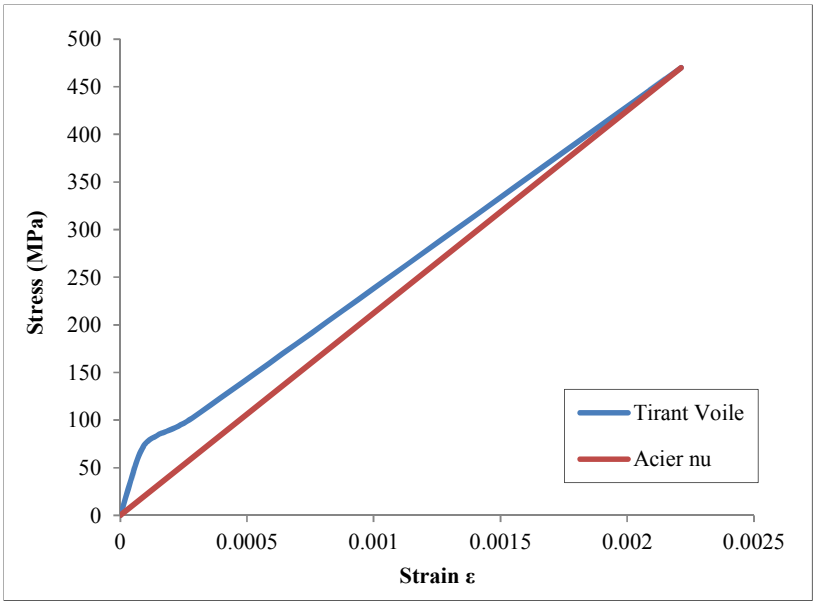

Figure 8. Fictitious behavior of steel in the effective stretched area of the wall SW21

The law of behavior of fictitious concrete relating to the homogenized section of the reinforced concrete tie rod ($\sigma_c = \frac{N}{(B-A_s)+(\eta A_s)}$ $o\grave{u}$ $\eta = \frac{E_s}{E_b}$) is then introduced into the CDP model in tension.

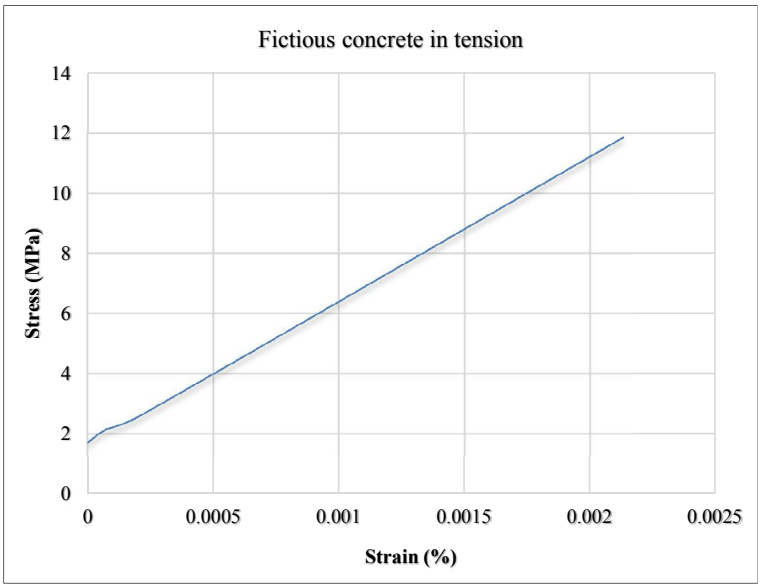

Figure 9. Uni-axial stress-strain curve in concrete traction (model2)

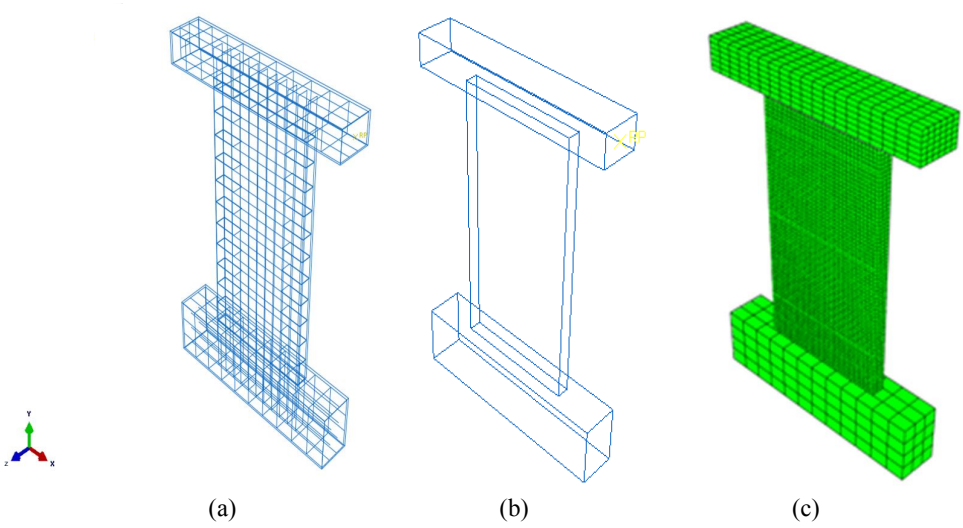

Figure 10. The different models (a) concrete wall with reinforcement (Model 1), (b) fictitious concrete wall without reinforcement (Model 2) and (c) EF mesh of concrete

4. Results and Discussion

Figure 11 shows that the finite element model 1 as well as the model 2 established from the fictitious behavior, reproduce in a very satisfactory manner the overall response of the wall SW21 observed experimentally. Model 2 (without direct reinforcement representation) gives very satisfactory results compared to the experimental one. This is due to the good estimation of the section adapted as the effective tensioned area of the wall.

It can be seen that on the experiment of Lefas and Kotsovos (1990) [9], the bending cracks appear starting from a loading step of 10KN. The response of the wall is then initially dominated by a behavior in bending. From 80KN, shear cracks begin to appear, the wall then behaves in combined bending-shear mode. The ultimate wall breaking force is observed for a load of 127KN. Wall failure is caused by crushing concrete in the zone of extreme pressure and tension with a concentration of shear cracks in the web of the wall.

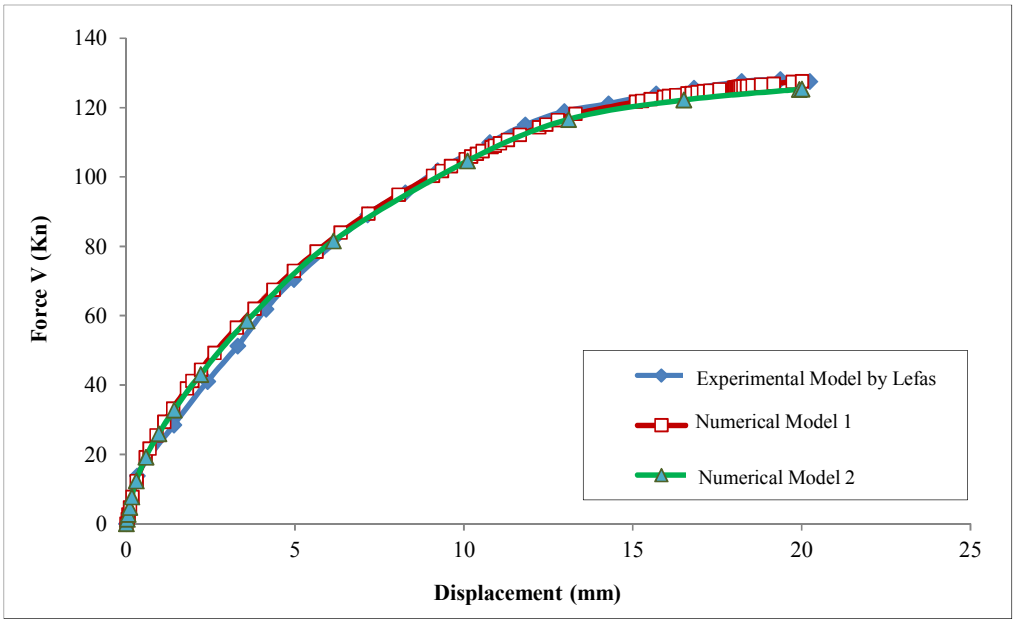

Figure 11. Comparison of experimental and numerical force-displacement curves of the reinforced concrete wall

Table 2 summarizes the various experimental ultimate values compared to the numerical values.

Table 2. Comparison between experimental and numerical results

Wall	Appearance of bending cracks		Appearance of shear cracks		Failure	
	Force (KN)	Displacement (mm)	Force (KN)	Displacement (mm)	Force (KN)	Displacement (mm)
Experimental result (Lefas)	10	0.32	80	5.81	127.5	20.6
Model 1	12.32	0.303	78.48	5.62	127.59	20
Model 2	12.318	0.289	81.51	6.21	125.33	20

Model 1 predicts the formation of flexural and shear cracks in concrete (Figure 12).

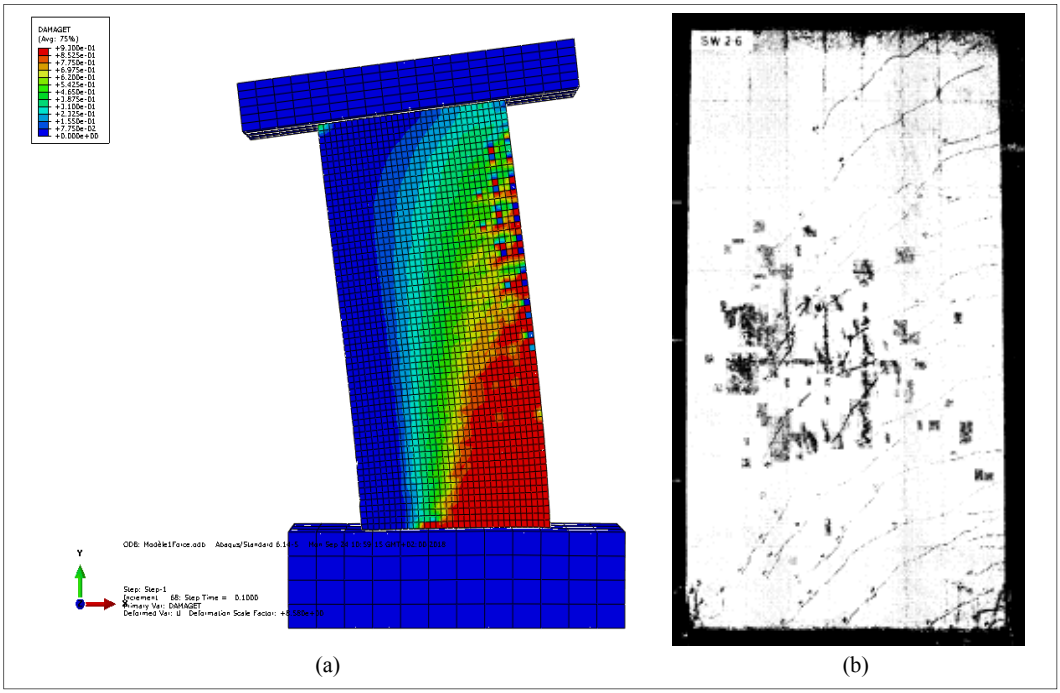

Figure 12. Comparison of the damage, (a) Model1 in tension, (b) Experimental

5. Conclusion

A finite element model taking into account the degradation of the tensile rigidity of reinforced concrete during cracking was presented and evaluated for a reinforced concrete wall in quasi-static loading. The model is quite simple and requires much less computation because it does not require the explicit representation of steel reinforcements to assess the overall behavior of reinforced concrete elements

Concerning reinforced concrete walls, the results of the comparison of the numerical simulations with the test results studied are rather satisfactory and the curves show that the two models (1 and 2) very faithfully reproduce the overall behavior of the reinforced concrete wall response. The contribution of concrete compared to steel is clearly demonstrated in the tensioned area. For the wall elements, by correctly estimating the percentage of steel in the tensioned area, that is to say judiciously defining the "tie rod" to be considered, the results of the proposed method are significantly close to the test results. However, the concrete section effectively tensed in bending must be clearly defined for any type of section so that the transposition of the “single tension tie rod” to the beam or wall is better suited. That said, and for all the numerical simulations carried out, model 2 offers the advantage of saving time, by doing without the representation of the reinforcements; as well as the ease and speed to reach convergence compared to a classical finite element modeling (model 1).

The main novelty of the model developed compared to the existing literature is that there is no need to model the steel reinforcement or the evolution of concrete damage under tension (as in existing models). Thanks to these characteristics, economic simulations (with regard to the calculation effort) are obtained without any divergence problem linked to the management of the progressive damage of concrete in tension. The model requires additional developments, in particular for its application on whole reinforced concrete structures and under different loadings (cyclic ...).

6. Funding

This work was funded by the PROFAS B+'s Scholarship. The financial support is gratefully acknowledged.

7. Acknowledgements

We thank the LAMOMS laboratory team, for their contribution to improve the work on the constitutive law part. We would also like to thank our colleagues from LERMAB Laboratory for their welcome and the resources made available throughout the duration of the scholarship.

8. Conflicts of Interest

The authors declare no conflict of interest.

9. Nomenclature

g	Relative slip between steel and concrete ($g = u_c - u_s$)	g_1	Value of the slip corresponding to the peak of the steel-concrete adhesion law (CEB)
τ	Bond slip shear between steel and concrete	τ_1	Maximum bond slip shear between steel and concrete
n	Equivalence coefficient $n = E_s/E_c$	p	Total perimeter of steel reinforcement
u_c, u_s	Respectively elongation of concrete and steel	A_s, A_c	Respectively, steel and concrete cross-sections
E_c, E_s	Respectively concrete and steel elastic moduli	N_t	External applied tensile force
α	Exponent of the slip-adhesion law proposed by the model code CEB 1990	γ	Total number of main cracks in the RC element
ρ	Steel reinforcement ratio	σ_c	Concrete normal stress
σ_e	Steel yield strength	σ_s	Steel tensile stress
σ_{sf}	Normal stress of the steel at the crack	L	Total length of the considered RC element
L_h	Length or sum of the lengths of the homogenized zones of the RC element	L_t	Sum of the total introduction lengths (l_t) of the RC element
l_0	disturbed length on either side of a crack($l_0 = \delta l_t$)	l_1	Effective introduction length when the slip g at the distance l_0 remains lower than g_1 (with $\lambda > 2l_t$)
l_t	Total introduction length	ε_e	Steel elastic strain limit
ε_m	Mean strain of the RC element	$\varepsilon_s, \varepsilon_c$	Respectively, steel and concrete strains
ε_{sf}	Steel strain in the cracked stage	ε_{sfa1}	Steel strain in the cracked stage corresponding to the introduction length l_{ta1}
$\varepsilon_{sm\lambda}$	Mean steel strain at crack stabilization corresponding to average crack spacing λ	$\varepsilon_{sm1}, \varepsilon_{cm1}$	Respectively mean steel and concrete strains corresponding along the introduction length l_1
$\varepsilon_{sma1}, \varepsilon_{cma1}$	Respectively mean steel and concrete strains corresponding along the introduction length l_{a1}	$\varepsilon_{smt1}, \varepsilon_{cmt1}$	Respectively mean steel and concrete strains corresponding along the introduction length l_{t1}
$\varepsilon_{smta1}, \varepsilon_{cmta1}$	Respectively mean steel and concrete strains corresponding along the introduction length l_{ta1}	$\varepsilon_{sr}, \varepsilon_{cr}$	Respectively steel and concrete strains at the first crack
λ, λ_1	Distance between two successive cracks corresponding, respectively, to the introduction lengths l_t and l_{t1}	$\bar{\lambda}$: (= 1,7 l_{tr})	Average spacing between two successive cracks at the crack stabilization state

10. References

[1] Saad, M., Y. Bouafia, and M. S. Kachi. "Contribution À L'évaluation D'ouverture Des Fissures Dans Les Éléments En Béton Armé." In Annales du Bâtiment et des Travaux Publics, no. 4, p. 102. Editions ESKA, (2014).

[2] Comité Euro-international du Béton, "CEB–FIP MODEL CODE 1990," Bulletin d'information, Juillet 1988. doi:10.1680/ceb-fipmc1990.35430.

[3] Ren, F.F., Z.J. Yang, J.F. Chen, and W.W. Chen. "An Analytical Analysis of the Full-Range Behaviour of Grouted Rockbolts Based on a Tri-Linear Bond-Slip Model." Construction and Building Materials 24, no. 3 (March 2010): 361–370. doi:10.1016/j.conbuildmat.2009.08.021.

[4] Saad, Monsieur. "Influence du pourcentage d'acier sur le comportement post-fissuration du béton armé en traction." PhD diss., Université de Tizi Ouzou-Mouloud Mammeri, (2011).

[5] Guo, Wei, Wei Fan, Xudong Shao, Dongjie Shen, and Baisheng Chen. "Constitutive Model of Ultra-High-Performance Fiber-Reinforced Concrete for Low-Velocity Impact Simulations." Composite Structures 185 (February 2018): 307–326. doi:10.1016/j.compstruct.2017.11.022.

[6] Mourlas, Christos, George Markou, and Manolis Papadrakakis. "3D Nonlinear Constitutive Modeling for Dynamic Analysis of Reinforced Concrete Structural Members." Procedia Engineering 199 (2017): 729–734. doi:10.1016/j.proeng.2017.09.030.

[7] Benakli, Sarah. "Modélisation du comportement non linéaire des structures en béton armé sous sollicitations quasi-statiques." PhD diss., Université Mouloud Mammeri de Tizi-Ouzou, Algérie, (2019).

[8] Benakli, S., Y. Bouafia, M. Oudjene, R. Boissière, and A. Khelil. "A Simplified and Fast Computational Finite Element Model for the Nonlinear Load-Displacement Behaviour of Reinforced Concrete Structures." Composite Structures 194 (June 2018): 468–477. doi:10.1016/j.compstruct.2018.03.070.

[9] I. Lefas and M. Kotsovos, "Strength and Deformation Characteristics of Reinforced Concrete Walls under Load Reversals." ACI Structural Journal 87, no. 6 (1990). doi:10.14359/2994.

[10] Lubliner, J., J. Oliver, S. Oller, and E. Oñate. "A Plastic-Damage Model for Concrete." International Journal of Solids and Structures 25, no. 3 (1989): 299–326. doi:10.1016/0020-7683(89)90050-4.

[11] K. S. Hibbit, ABAQUS, Theory Manual, Version 6.2, (2000).

[12] Lee, Jeeho, and Gregory L. Fenves. "Plastic-damage model for cyclic loading of concrete structures." Journal of engineering mechanics 124, no. 8 (1998): 892-900. doi:10.1061/(asce)0733-9399(1998)124:8(892).

[13] S. Rossier, "Analyse numérique non linéaire des structures en béton à parois minces," Ecole polytechnique fédérale de Lausanne, Suisse, (1999).